DOI: 10.1002/cmdc.200600286

G-Quadruplex Recognition by Quinacridines: a SAR, NMR, and Biological Study

Candide Hounsou,[a] Lionel Guittat,[b] David Monchaud,[a] Muriel Jourdan,[c] Nicolas Saettel,[a] Jean-Louis Mergny,[b] and Marie-Paule Teulade-Fichou*[a]

The synthesis of a novel group of quinacridine-based ligands (MMQs) is described along with an evaluation of their G-quadruplex binding properties. A set of biophysical assays was applied to characterize their interaction with DNA quadruplexes: FRET–melting experiments and equilibrium microdialysis were used to evaluate their quadruplex affinity and their ability to discriminate quadruplexes across a broad panel of DNA structures. All data collected support the proposed model of interaction of these compounds with G-quadruplexes, which is furthermore confirmed by a solution structure determined by 2D NMR experiments. Finally, the activity of the MMQ series against tumor cell growth is reported, and the data support the potential of quadruplex-interactive compounds for use in anticancer approaches.

Introduction

Telomeres are nucleoprotein complexes that cap and protect the eukaryotic chromosomes.[1] The terminal part of the telomere is composed of a G-rich single-stranded nucleotide sequence (linear repeats of $d[T_2AG_3]$), which is currently a topic of widespread scientific interest because it is essential for telomere integrity and may fold into G-quadruplexes.[2] This particular DNA arrangement is composed of three stacked G-tetrads (four Hoogsteen-paired coplanar guanine residues) linked together by interconnecting loops with different spatial arrangements depending on the nature of the quadruplex structure.[3] Designing molecules that are able to target and interact with G-tetrads is a challenging yet promising anticancer strategy. Indeed, molecules that interact with G-tetrads stabilize the quadruplex structure which leads to telomere dysfunction through disruption of protein–telomere interactions[4] and in particular, a modulation of the association with telomerase. For cancer cells, this enzyme is pivotal because it is deeply involved in the immortalization process by preventing the natural erosion of telomeres. Interestingly, this enzyme is active in most (~85%) cancer cells, and inactive, or weakly active, in most normal somatic cells.[5] Perturbation of telomerase activity is thus a promising therapeutic strategy.[6]

This novel approach has led to a considerable interest in the identification of new chemical series of quadruplex ligands.[7] Among them, we recently reported a series of quinacridines as potentially powerful candidates.[8] Compound **1** (also known as MMQ_1,[8c,d] Figure 1) is the leading compound of the MMQ (mono-*meta*-quinacridine) series; it exhibits good quadruplex stabilization properties and a fair selectivity for quadruplex over duplex DNA.[8]

On the basis of the crystal structure determined for a disubstituted acridine–quadruplex complex,[9] a model of interaction between **1** and G-quadruplex DNA can be postulated. The complex is probably stabilized by π-stacking interactions between the fused pentacyclic aromatic core of the molecule and an accessible G-tetrad, coupled with electrostatic interactions between the protonated side chains and the negatively charged quadruplex grooves. To validate this assumption, we report herein a complete structure–activity relationship study based on chemical derivatization and the subsequent evaluation of this new series of ligands for quadruplex recognition and biological activity. To gain further insight into the quinacridine–quadruplex binding mode, a 2D NMR determination of the solution structure of complex of **1** with a tetramolecular quadruplex is also reported.

Results

Chemistry

A wide chemical declination program was undertaken around the quinacridine skeleton to determine the structural features

[a] *C. Hounsou, Dr. D. Monchaud,[+] Dr. N. Saettel, Dr. M.-P. Teulade-Fichou[+]*
Laboratoire de Chimie des Interactions Moléculaires, CNRS UPR 285
Collège de France, 11, place Marcellin Berthelot, 75005 Paris (France)
E-mail: marie-paule.teulade-fichou@curie.fr

[b] *L. Guittat, Dr. J.-L. Mergny*
Laboratoire de Biophysique, INSERM U565 CNRS UMR 5153
Muséum National d'Histoire Naturelle, USM503, 43, rue Cuvier, 75005 Paris (France)

[c] *Dr. M. Jourdan*
Département de Chimie Moléculaire, UMR-5250, ICMG FR-2607, CNRS
301 rue de la Chimie, Bat. Chimie Recherche, 38041 Grenoble, Cedex 9 (France)

[+] *Current address:*
Institut Curie, Section Recherche, CNRS UMR176
Centre Universitaire Paris XI, Bâtiment 110, 91405 Orsay (France)
Fax: (+33) 1-69-07-53-81

Supporting information for this article is available on the WWW under http://www.chemmedchem.org or from the author.

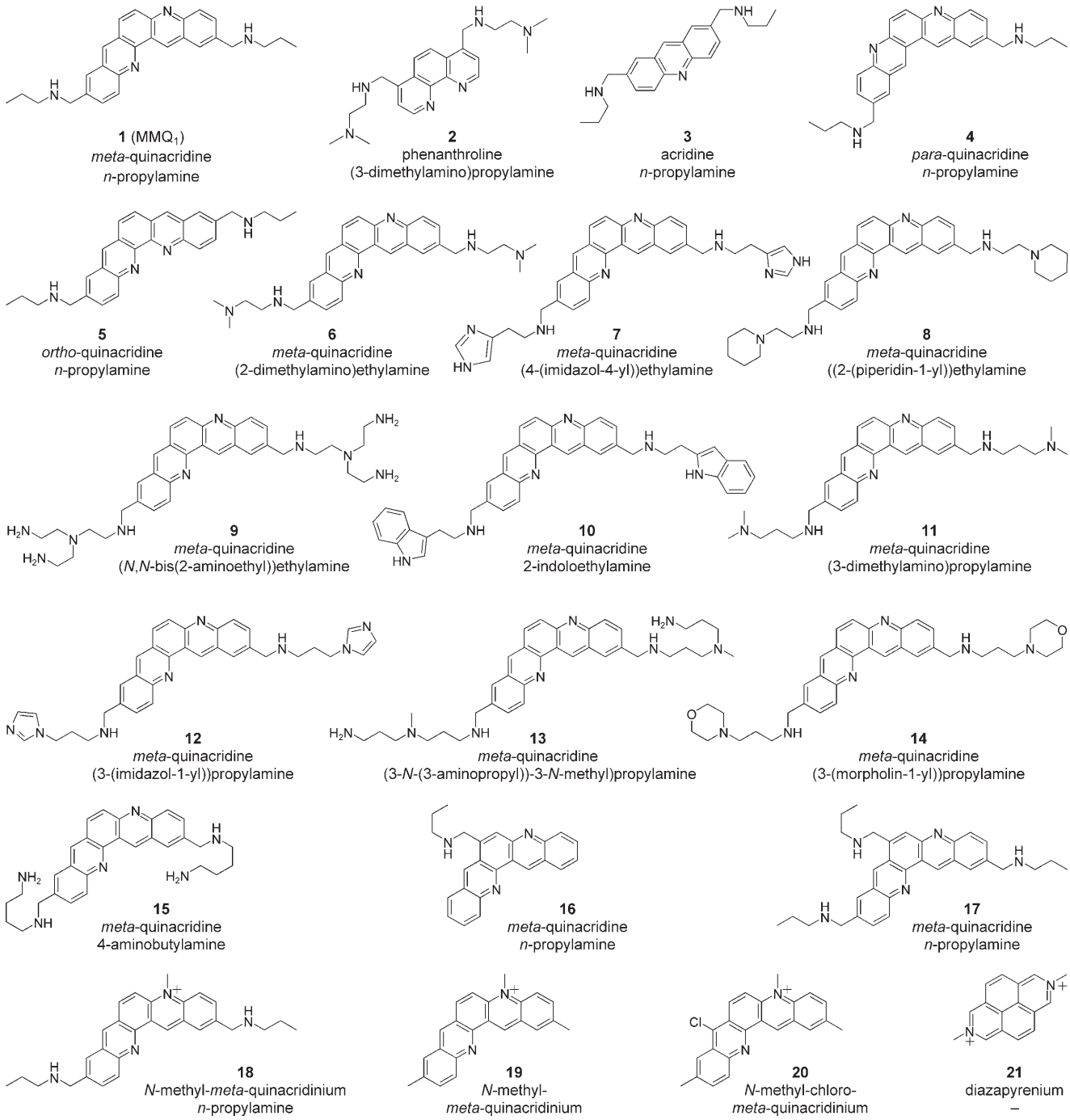

Figure 1. Structures of compounds **1**–**21**; the nature of the aromatic core (quinacridine, phenanthroline, acridine, or diazapyrenium) and amine side chains is indicated.

that govern quadruplex recognition. Structures of the 21 molecules studied in the present work are summarized in Figure 1.

Detailed syntheses have been previously reported for **1**–**5**, **11**, and **21**, as well as for the intermediates **22**–**25** (Schemes 1 and 2).[8,10–12] The synthetic pathways of the newly synthesized compounds are briefly presented below.

Synthesis of disubstituted and *N*-methylated quinacridines

The disubstituted MMQs (compounds **6**–**15**) are obtained by the classical two-step procedure reported for **1** from dimethylquinacridine **22** (Scheme 1): a SeO_2-mediated oxidation of aromatic methyl groups (60% yield) leads to bis-carboxaldehyde derivatives, which are subsequently converted into amino derivatives by a $NaBH_4$-mediated reductive amination (14–60% yield, depending on the nature of the amine).

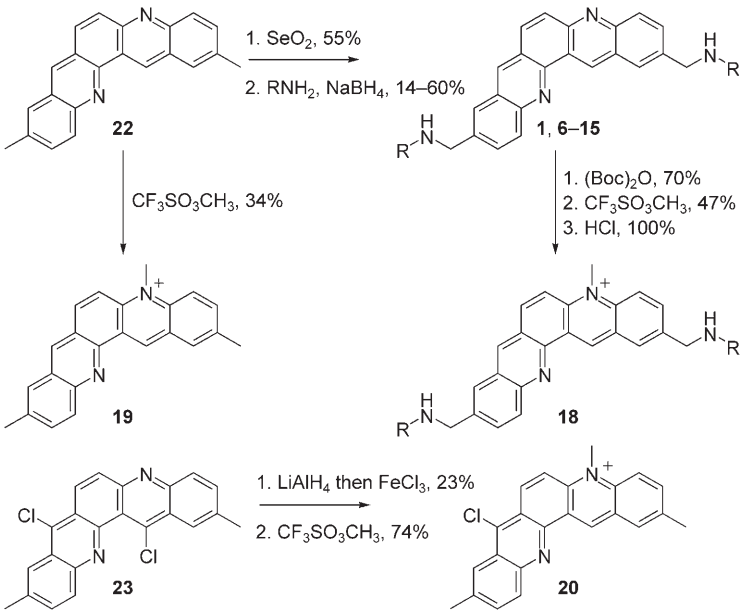

Scheme 1. Synthesis of disubstituted MMQs **1**, **6**–**15** and *N*-methylated MMQs **18**–**20**.

Concerning the *N*-methylated MMQs **18**–**20**, selective monomethylation reactions were attempted to benefit from the putative nonequivalence of the two cyclic nitrogen atoms in terms of reactivity and accessibility. Thus, quaternarization of **22** using methyl trifluoromethanesulfonate produced the monomethylated product **19** directly, although in moderate yield (34% after purification). Obtaining **18** required a three-step procedure based on a protection (or the secondary amines situated on the side-arms)/methylation (or the intracyclic nitrogen)/deprotection sequence (47% chemical yield, Scheme 1). In both cases the bis-quaternary ammonium derivative was formed as a by-product, but was easily removed by column chromatography. The nonequivalence of the two nitrogen atoms was also exploited to perform a controlled hemi-reduction reaction. Indeed, the hemi-reduction of the dichloroquinacridine derivative **23** was achieved through stoichiometric control of the amount of $LiAlH_4$ (2 equiv instead of 8 equiv for the double reduction). Compound **20** was thus obtained after methylation of the "external" cyclic nitrogen atom (16% chemical yield over three steps). The hemi-reduction of **23** is not only favored by the difference in reactivity of the two cyclic nitrogen atoms, but may also be preferentially oriented by a possible interaction of $LiAlH_4$ with the "internal" nitrogen atom. Interestingly, in this case, the monomethylation step was more efficient (74% chemical yield) owing to an increase of the difference in electronic properties of the two nitrogen atoms by deactivation of the 'internal' nitrogen by the chlorine atom located in the *para* position.

Synthesis of mono- and trisubstituted quinacridines

A similar two-step protocol (oxidation/reductive amination) was followed for the synthesis of mono- and trisubstituted quinacridines **16** and **17** (respectively from monomethylquinacridine **24** and trimethylquinacridine **25**, Scheme 2), which results in moderate product yield.

FRET–melting assay

The quality of the association between quinacridines and quadruplex DNA was first evaluated by FRET–melting experiments and thereafter quantified by $\Delta T_{1/2}$ values.[13] FRET results are summarized in Table 1 together with in situ estimated charges.[14]

The quinacridine motif

The initial synthetic efforts were aimed at probing the influence of both the aromatic surface and the cyclic nitrogen positions. As shown in Table 1, decreasing the aromatic surface (from pentacyclic quinacridine **1** to tricyclic phenanthroline **2** or acridine unit **3**) leads to a near complete loss of quadruplex stabilization ($\Delta T_{1/2} = 12.5$, 1.5, and 0 °C for **1**, **2**, and **3**, respectively). Such an effect is proportional to the area of aromatic surfaces in contact, which indicates that π-stacking interactions are the dominant aspect in controlling the ligand–quadruplex association. The modification of the relative positions of the two ring nitrogen atoms has only a slight effect on $\Delta T_{1/2}$, as shown by FRET experiments carried out with disubstituted *meta*-, *para*-, and *ortho*-quinacridines **1**, **4**, and **5**. These results suggest that the ring nitrogens play only a very minor role in binding to the quadruplex, and underscores the size and crescent shape of the quinacridine ligands as their most influential structural features. Furthermore, these experiments indicate the equivalence of positions 2/3 and 10/11 of the quinacridine ring for side chain connection.

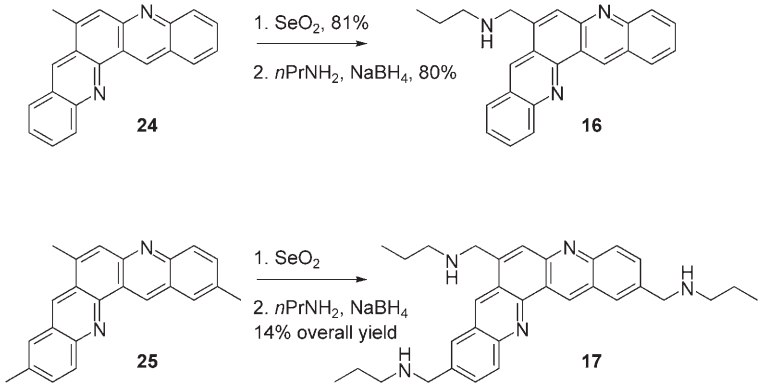

Scheme 2. Synthesis of mono- and trisubstituted MMQs **16** and **17**, respectively.

Table 1. Estimated charge[a] and FRET–melting results for compounds **1**–**21**.

Ligand	Charge	$\Delta T_{1/2}$ [°C][b]	Ligand	Charge	$\Delta T_{1/2}$ [°C][b]
1	2+	+12.5	**12**	1–2+	+15.0
2	3+	+1.5	**13**	5–6+	+21.0
3	2+	0	**14**	2–3+	+7.0
4	2+	+11.5	**15**	4+	+18.0
5	2+	+12.5	**16**	1+	+1.5
6	2+	+9.8	**17**	3+	+19.0
7	3+	+19.7	**18**	3+	+21.5
8	2+	+8.1	**19**	1+	+10.0
9	5+	>30	**20**	1+	+16.0
10	1–2+	+8.4	**21**	2+	0
11	3+	+19.7			

[a] See reference [14] for charge estimation. [b] $\Delta T_{1/2} = [T_{1/2}(\text{quadruplex DNA + ligand})] - [T_{1/2}(\text{quadruplex DNA})]$, determined with standard FRET–melting conditions (0.2 μM F21T and 1 μM ligand; see reference [13]).

The nature of the side chain

The 2,10-disubstituted *meta*-quinacridine pattern (from **1**) was kept as a model for evaluating the influence of the nature of the side chain. As shown in Figure 1, various amines have been introduced as side chain groups (**6**–**10**: ethyl-, **1** and **11**–**14**: propyl-, and **15**: butylamine derivatives), with a representative panel of substituents: **1**: H, **6** and **11**: dimethylamino, **7** and **12**: imidazolo, **8**: cyclohexyl, **9**: bis(2-aminoethyl)amino, **10**: indolo, **13**: (3-aminopropyl)methylamino, **14**: morpholino, and **15**: amino groups. The global charge brought by the side chains has a strong influence on the binding, as highly cationic species strongly stabilize the quadruplex structure (for example, $\Delta T_{1/2} = 10$, 12.5, 19.7, and >30 °C for compounds **19**, **1**, **11**, and **9** bearing 1, 2, 3, and 5 cationic charges, respectively). In our hands, the use of a ligand with at least three charges results in a $\Delta T_{1/2}$ value higher than 19 °C. This observation means that the control of electrostatic parameters is important for insuring good quadruplex–ligand associations.

The side chain number

The introduction of a third groove-interacting side chain has already proven its efficiency for acridine ligands.[15] Such a possibility exists on the central ring of the quinacridine (Scheme 2). As listed in Table 1, FRET experiments performed with quinacridines bearing one, two, and three propylamine side chains lead to increasing $\Delta T_{1/2}$ values (from 1.5, 12.5, to 19.0 °C for **16**, **1**, and **17**, respectively). Such an enhancement in affinity could result from synergic effects between an optimized quadruplex interaction and an increase of the global molecular charge (1, 2, and 3+ for **16**, **1**, and **17**, respectively).

The electronic density of the aromatic surface

G-tetrads can be considered as a large and electron-rich aromatic surfaces, thus a diminution of the electronic density of the quinacridine unit might be expected to have a strong impact on the π-stacking interaction between the G-tetrads and the ligand. To this end, the quaternarization of one cyclic nitrogen atom of the quinacridine unit was achieved. As listed in Table 1, a remarkable improvement in quadruplex stabilization was obtained with the quaternarization of **1** (12.5 and 21.5 °C for **1** and **18**, respectively). Although the higher cationic charge of **18** can contribute to this improvement, this is most likely due to enhancement of the π-stacking interaction by the depletion of the electronic density of the ligand. This is further confirmed by the introduction of a strong electron-withdrawing element (chlorine atom), which induces a strong enhancement in $\Delta T_{1/2}$ (10 and 16 °C for **19** and **20**, respectively) without modifying the ligand charge. Finally, the absence of effect with the linear biscationic diazapyrenium **21** in comparison with the good performances of **19** and **20** clearly indicates that the strength of the quinacridine–quadruplex association relies heavily on the particular crescent shape of the quinacridine ring.

Altogether, these results strongly suggest that π-stacking and electrostatic interactions govern the association of the MMQ series with the quadruplex. Additionally, a comparison of the results obtained with the three monocationic compounds **16**, **19**, and **20** underscores that the balance between these parameters can be fine-tuned, as a positive charge on the heterocycle appears to be much more efficient than a charge outside the heterocycle.

To gain further insight concerning the mode of association between MMQs and G-quadruplexes, NMR studies were carried out with **1** and a quadruplex. However, because the intramolecular quadruplex used in the FRET experiments gave poor results (broad NMR signals in complex with **1**), we chose a tetramolecular quadruplex in which the DNA sequence has been a successful substrate for the investigation of other ligand interactions.[16]

NMR studies

This technique has been successfully used to elucidate the mode of interaction of ligands such as PIPER, RHPS4, and distamycin with a tetramolecular quadruplex,[16] TMPyP4 with an intramolecular quadruplex,[17] and quinobenzoxazine with both structures.[18] In all cases, stacking on the surface of G-quartets has been evidenced excluding the possibility of true intercala-

tion between stacks of G-tetrads. NMR spectroscopy is particularly powerful in determination of the precise site of interaction and also for establishing the stoichiometry of the complex. In the present case, 1D NMR titration experiments clearly showed a 2:1 stoichiometry for binding of **1** to the tetramolecular quadruplex $[d(T_2AG_3T)]_4$ derived from human telomere DNA sequences and noted hereafter as $[d(T_1T_2A_3G_4G_5G_6T_7)]_4$ (Figures 2 A and B and Supporting Information). The precise position of the two ligands within the quadruplex was then investigated using 2D NMR experiments. Chemical-shift mapping revealed an upfield shift of the imino exchangeable protons of G_4 and G_6 (see Supporting Information), and detection of characteristic NH/G_4–NH/G_5 and NH/G_5–NH/G_6 NOE cross-peaks strongly suggest that the ligand stacks over G_4 and G_6 bases, with one molecule located between the bases of A_3 and G_4, and the other between G_6 and T_7 steps (Figure 2 B). G-tetrads, observed in the unbound quadruplex, are conserved in the complex and are not disrupted by the stacking of the drug. We indeed identified unambiguous characteristics of inter-strand NOE (for example, between G imino protons with their own G-H8 proton and with their 5′-flanking base G-H8 proton) consistent only with the presence of G-tetrads. However, there was no experimental evidence of A-tetrads, although they were formed in the free quadruplex. The binding of the drug, in fact, causes slight structural distortions over theses bases.

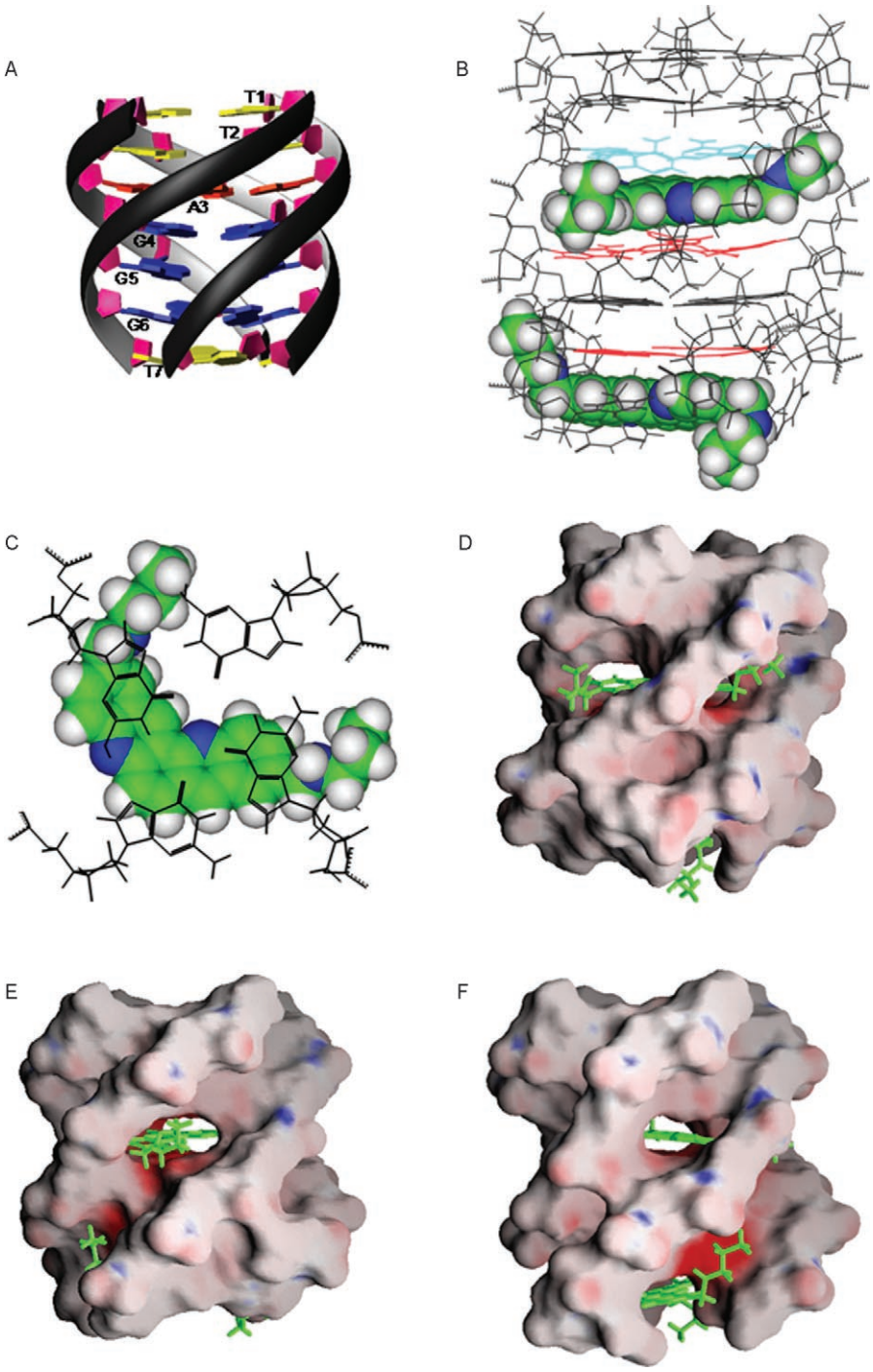

Figure 2. A) Representation of the tetramolecular quadruplex $(d[T_2AG_3T])_4$ with base numbering (thymine residues appear in yellow, adenine in red, and guanine in blue); B) Side view of the 2:1 **1**–quadruplex complex: G_4 and G_6 quartets appear in red, and A_3 bases in blue; C) π-stacking interaction between the G_4 tetrad and **1**; D)–F) Electrostatic surface of the quadruplex with positive and negative potentials colored in blue and red, respectively. Visualization of electrostatic interactions between the positively charged side chains of **1** and negatively charged quadruplex grooves (obtained with GRASP program[19]).

Few intermolecular NOE observed between the ligand and A_3 and G_4 protons, as well as G_6 protons further confirm the mode of association within the quadruplex (see Supporting Information). The complex was then modeled using a molecular dynamics simulation in vacuo under experimental restraints. Owing to the highly dynamic nature of the complex and a limited number of NOE signals, calculations were restricted to the two binding sites only (see Experimental Section), and a precise structure could not be determined. However, we are able to propose a model with enough accuracy that shows π-stacking interactions between the ligand and the G quartet, with the cationic side chains clearly directed toward the negatively charged quadruplex

grooves (Figure 2C). The double anchorage in the grooves is fully confirmed by GRASP visualizations[19] of the complex (Figure 2D–F), which show that the side-arms of **1** fit snugly inside red pockets of the quadruplex grooves, which symbolize regions of highly negative potential. Electrostatic interactions with the grooves are thus highly involved in the stabilization of the complex. Albeit frequently hypothesized, interactions of ligand side chains with quadruplex grooves have been structurally characterized only in a few cases.[16a,b,18,20]

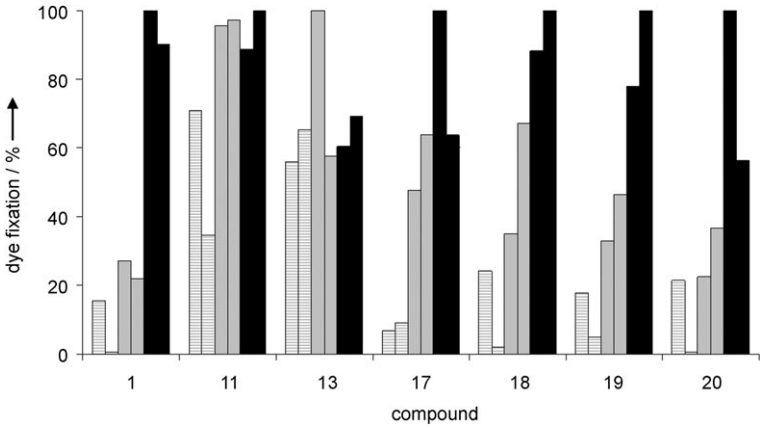

Figure 3. Normalized fixation of quinacridines **1**, **11**, **13**, and **17**–**20** onto single-stranded DNA (dashed gray, poly-d(A) (left) and poly-d(T) (right)), duplex DNA (solid gray, ds26 (self complementary sequence 5′-$CA_2TCG_2ATCGA_2T_2CGATC_2GAT_2G$-3′ (left)) and calf thymus DNA (right)), and quadruplex DNA (black, 24G20 (5′-$T_2G_{20}T_2$-3′ (left)) and 22AG (5′-$AG_3[T_2AG_3]_3$-3′[8] (right)) established by equilibrium microdialysis.

Quadruplex selectivity

As demonstrated previously, highly cationic ligands greatly stabilize the quadruplex structure upon melting. Nevertheless, the increase in molecular charge could have a cost in terms of quadruplex selectivity. To investigate the influence of ligand charge, we used the equilibrium microdialysis experiment that is one of the most discriminating tests for this purpose.[21] Ligands are exposed to various DNA structures; their selectivity is then determined from the proportion of fixed ligand on each DNA structure. A representative panel of quinacridines has been tested: disubstituted **1** (2+, $\Delta T_{1/2} = 12.5\,^{\circ}C$), **11** (3+, 19.7 °C) and **13** (5–6+, 21 °C), trisubstituted **17** (3+, 19 °C), and the N-methylated quinacridines **18** (3+, 21.5 °C), **19** (1+, 10 °C) and **20** (1+, 16 °C). Results are presented in Figure 3.

The results obtained underscore the high selectivity of compound **1**. Indeed, they indicate a clear preference for fixation onto quadruplex DNA relative to single-stranded or duplex DNA (with a minimum of 6.5-fold and 3.3-fold preference for fixation onto quadruplex over single-stranded and duplex DNA, respectively). On the other hand, compounds **11** and **13** (both highly cationic) appear totally unselective. Similarly, the trisubstituted quinacridine **17** (3+) binds only with poor selectivity to quadruplex, although it binds very poorly to single-stranded DNA. Finally, N-methylated quinacridines **18**–**20** show good selectivity, particularly compound **20**, which displays up to 4.4-fold preference for quadruplex over duplex DNA.

These results are consistent with data previously obtained from the new G4-FID assay that allows estimation of quadruplex versus duplex selectivity by displacement of the fluorescent DNA probe, thiazole orange.[22] Indeed, this test confirmed the selectivity of the N-methylated quinacridine **20**, which exhibits a high preference for 22AG (see the legend of Figure 3) relative to a 17-bp duplex.[22] In good agreement with the microdialysis assay, compounds **11** and **13** were also shown to have poor quadruplex over duplex selectivity.

To gain further insight into quadruplex selectivity, competitive FRET experiments were carried out with the same series of ligands.[10,13,23] In these experiments, the labeled oligonucleotide F21T is melted in the presence of unlabeled double-stranded (ds) DNA competitor in excess (ds26; 15 and 50-fold excess, see Supporting Information). The decrease in stabilization is expressed as a percentage of the $\Delta T_{1/2}$ measured in the absence of competitor (Figure 4). Globally, the trends observed in the previous assays are confirmed: compounds **1** and **18**–**20** display good to moderate selectivity; **20** appears to be the most resistant, as its quadruplex stabilization is maintained to 58% under these conditions. Similarly, highly cationic derivatives **13** and **17** were poor selectors as demonstrated by the dramatic decrease (>90%) in the presence of duplex competitor. Unexpectedly, compound **11** demonstrates fair resistance, thus appearing more selective than anticipated. This discrepancy probably originates from the difference in experimental conditions between the two assays, considering that melting measurements only indirectly reflect binding affinities. To complete the biophysical data, biological investigations were conducted with a representative panel of quinacridine ligands.

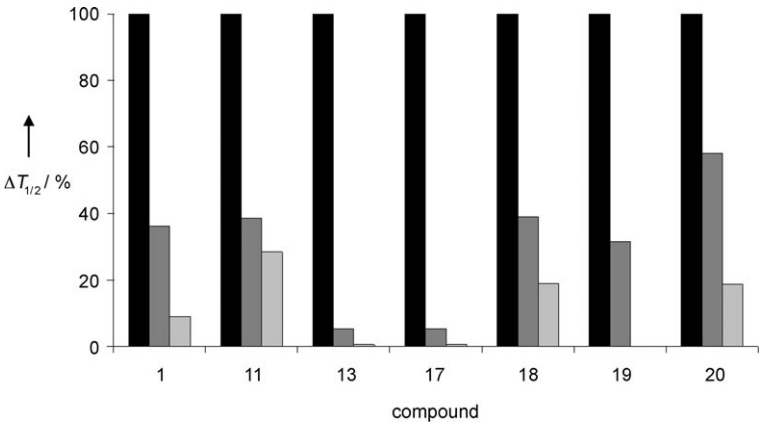

Figure 4. Normalized FRET results for compounds **1**, **11**, **13**, and **17**–**20** (1 μM), without (black) and with 15-fold (3 μM; dark gray) or 50-fold (10 μM; light gray) excess of duplex DNA competitor (ds26).

Biological activity

To evaluate the biological activity of this series of molecules, their effect in vitro on short-term inhibition of cell growth (assumed to mediated through a strong G-quadruplex interaction) was assessed on the A431 cell line[15a] by using the MTT colorimetric assay.[24] Results for compounds **1**, **6**, **7**, **9**, **11**–**13**, **15**, and **18**–**20** are presented in Figure 5 as concentrations required to inhibit cell growth by 50% (IC_{50}).

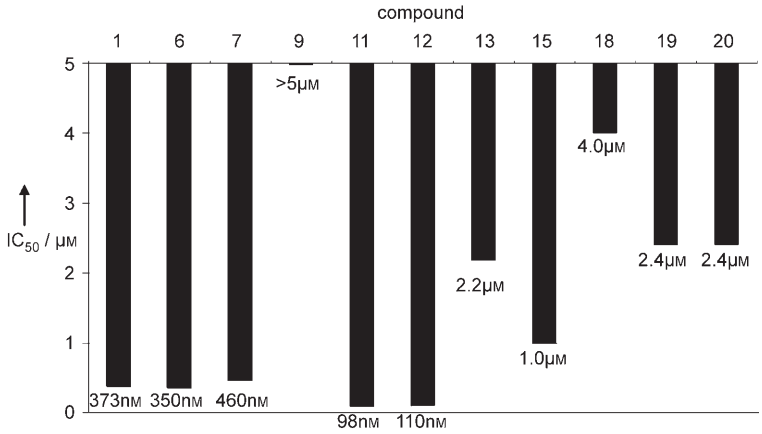

Figure 5. Cytotoxicity of compounds **1**, **6**, **7**, **9**, **11**–**13**, **15** and **18**–**20** toward the A431 cell line.

MMQs **1**, **6**, **7**, **11**, and **12** appear to be the most active compounds (IC_{50} values below 0.5 μM). The suitable molecular charge for good efficiency thus appears to be between 1–2+ (**12**, IC_{50} = 110 nM) and 3+ (**11**, IC_{50} = 98 nM). Quinacridines with higher cationic charges (compounds **9** (5+) and **13** (5–6+)) are moderate to poor inhibitors under these test conditions, probably because their charge severely limits cellular uptake. In contrast, ligands with minimal cationic charge (compounds **19** and **20** (1+)) present only moderate toxicity (IC_{50} = 2.4 μM).

Discussion

The quinacridines reported herein were thoroughly studied for their quadruplex binding properties, in terms of both quadruplex affinity and their ability to discriminate quadruplex over duplex DNA. These studies confirm that the quinacridine motif (with its intrinsic crescent shape), coupled with amine side-arms protonated at physiological pH, is highly valuable for the design of quadruplex-interactive agents. Different structural parameters were studied (the nature and electronic density of the central aromatic core, as well as the nature and number of side chains), and the subsequent impact on quadruplex recognition was evaluated with biophysical (FRET, microdialysis, G4-FID) and biological (short-term inhibition of cell growth) assays. Interestingly, structure–activity relationship analyses allow us to design a MMQ–quadruplex association mode that has been fully confirmed by NMR studies of the complex of compound **1** with the tetramolecular quadruplex $[d(T_2AG_3T)]_4$. This NMR structure illustrates and underscores the critical influence of cationic side-arms on the fixation of the ligand, and their role for optimizing quadruplex stabilization.

Two series of ligands have emerged as possible candidates from the biophysical studies: the disubstituted (compounds **1**, **6**–**15**) and N-methylated (compounds **18**–**20**) quinacridines. These ligands combine affinity and selectivity, which are the two essential criteria in the selection process. In this regard, disubstituted **11** represents a minor candidate as a result of its low quadruplex versus duplex selectivity, yet it is highly active against cancer cell growth (IC_{50} = 98 nM). Also unexpected is the low cellular activity (IC_{50} > 2 μM) of the N-methylated quinacridines **18**–**20** which may be attributed to uncontrollable pharmacokinetic parameters. In summary, the disubstituted MMQs that bear a moderate cationic charge (2+) represent a good compromise, because they fulfill the criteria of biophysical and biological evaluations (high affinity, good selectivity, and IC_{50} values in the range of 300–500 nM).

Altogether, our results demonstrate the problems that must be bypassed during a quadruplex ligand selection process. In particular, great care has to be taken when correlating the results of biophysical and biological evaluations, thereby emphasizing the difficulty in predicting the effectiveness of a particular quadruplex-interactive compound in a cell-based assay. In terms of target recognition, molecular charge and electronic density appear highly valuable parameters to control, but also particularly subtle to balance. In that sense, and despite their biologically contrasting profiles, N-methylated quinacridines appear as good candidates for further structure–activity relationship studies. Studies are currently being conducted to understand and circumvent the origins of their moderate biological response.

Conclusions

In conclusion, when taken with the reports of the existence of quadruplexes in vivo,[25] the present study supports the anticancer approach based on the interaction between quadruplexes and small synthetic ligands. The members of the MMQ family appear to be very reliable candidates, and they open broad perspectives through the wide range of possibilities in terms of their structural diversity. In particular, the study presented herein points out the required structural features of MMQs to be further exploited to optimize their potential as anticancer agents. In particular, further research concerning ligands of type **1** and **20** are currently being undertaken. Finally, thanks to the NMR elucidation of the **1**–quadruplex interaction, this study also may provide future points for the rational design of more selective G-quadruplex ligands based on DNA groove interactions.

Experimental Section

Equilibrium microdialysis,[21] fluorescent intercalator displacement (G4-FID),[22] fluorescence resonance energy transfer (FRET),[13,23] and MTT colorimetric assays[24] were carried out following previously reported procedures.

Chemistry: NMR spectra were recorded at 200 MHz on a Bruker Aspect 3000, at 300 MHz on a Bruker Avance 300, and at 500 MHz on a Varian Unity+ using TMS as internal standard. Deuterated solvents ($CDCl_3$, [D_6]DMSO, [D_4]MeOD, CD_2Cl_2, D_2O) were purchased from SDS. The following abbreviations are used: singlet (s), doublet (d), doubled doublet (dd), triplet (t) and multiplet (m). Mass spectrometry services were provided by the Laboratoire de Chimie Structurale Organique et Biologique (Université Pierre et Marie Curie, Paris). Microanalyses were provided by the I.C.S.N. (Institut de Chimie des Substances Naturelles, Gif-sur-Yvette) microanalysis service centre. UV/Vis experiments were carried out on a Beckman DU640 or a Uvikon XL Secomam spectrophotometer. Fluorescence measurements were performed on a FluoroMax-3 spectrofluorimeter (Jobin-Yvon). IR spectra were collected on a Bruker Vector 22 instrument. Melting points (mp, uncorrected) were determined on an Electrothermal 9100 instrument. TLC analysis was carried out on silica gel (Merck 60F_{254}) with visualization at 254 and 366 nm. Preparative flash chromatography was carried out with Merck silica gel (Si 60, 40–63 μm). Reagents and chemicals were purchased from Sigma–Aldrich, unless otherwise stated. Solvents were purchased from SDS. Dichloromethane (CH_2Cl_2), chloroform ($CHCl_3$), methanol (MeOH), and 1,2-dichloroethane ($ClCH_2CH_2Cl$) were distilled from calcium hydride. Tetrahydrofuran (THF) was distilled from sodium. Naphthalene, ethanol (EtOH), and pentane were used without purification. The synthesis of compounds **1**–**5**, **11**, and **21** was reported previously, as well as that of the intermediates **22**–**25**.[8,10–12]

General procedure for the synthesis of MMQs 1, 6–15: Dimethylquinacridine **22** was converted into the bis-carboxaldehyde derivative upon treatment with selenium dioxide (SeO_2): a mixture of dimethylquinacridine **22** (500 mg, 1.64 mmol), naphthalene (10 g), and SeO_2 (400 mg, 3.62 mmol) was heated at reflux and stirred for 2.5 h. The mixture was then cooled to 70 °C and filtered. The solid collected was thoroughly washed with a mixture of CH_3OH/CH_2Cl_2 (1:4); solvents were mixed together and removed under reduced pressure. The solid was washed with pentane (3 times); after the solvent was removed, the solid was dried under reduced pressure. Bis-carboxaldehyde derivatives were obtained as a yellow powder (55% chemical yield). mp: (dec) > 350 °C; ^{1}H NMR (200 MHz, $CDCl_3$/CD_3OD 5:1): δ = 8.28–8.34 (m, 6H), 8.72 (s, 2H), 9.78 (s, 2H), 10.25 ppm (s, 2H); IR (nujol): $\tilde{\nu}$ = 1697, 1615 cm^{-1}; anal. calcd for $C_{22}H_{12}N_2O_2$, 0.22 $CHCl_3$: C 73.60, H 3.40, N 7.73, found: C 73.63, H 3.47, N 7.59.

The amine to be introduced as side chain was added to a solution of the previously prepared bis-carboxaldehyde derivatives in CH_3OH/CH_2Cl_2 (1:4). The mixture was stirred at room temperature (for **1**, **6**, **8**, **9**, **11**, **13**, and **15**) or under solvent reflux (for **7**, **10**, **12**, and **14**) until the complete disappearance of the aldehyde signals, as monitored by ^{1}H NMR. The solvents were distilled off, and the crude diimine was dissolved in methanol, then cooled to 0 °C. $NaBH_4$ (4 equiv) was added, and the solution was stirred at 0 °C for 2 h and at room temperature for 30 min. The solvent was distilled off, and water (2 mL) was added. The product was then extracted with CH_2Cl_2. The organic layer was dried over $MgSO_4$, filtered, and evaporated. The residue obtained was dissolved in CH_3OH, and HCl (1 N) was added to give a chloride salt, which was precipitated by the addition of THF. The salt was finally crystallized from EtOH/HCl (1 N) to yield the desired product in pure form.

2,10-Di-[(2-dimethylaminoethyl)aminomethyl]dibenzo[*b,j*]-[*1,7*]phenanthroline 6 was obtained from dibenzo[*b,j*]-[*1,7*]phenanthroline-2,10-dicarboxaldehyde (100 mg, 0.297 mmol) and 2-dimethylaminoethylamine (3.26 mL, 29.7 mmol) to yield 60 mg of a yellow–green powder (28%). Salt decomposition: 200 °C; ^{1}H NMR (200 MHz, D_2O/DCl): δ = 2.9 (s, 12H), 3.55 (sext, J = 7.9 Hz, 8H), 4.49 (s, 2H), 4.54 (s, 2H), 7.75 (d, J = 9.38 Hz, 1H), 7.85 (d, J = 9.02 Hz, 1H), 7.97 (d, J = 8.52 Hz, 1H), 8.05 (s, 1H), 8.1 (s, 1H), 8.14 (s, 1H), 8.22 (d, J = 8.64 Hz, 1H), 8.37 (s, 1H), 8.78 (s, 1H), 10.03 ppm (s, 1H); MS (ESI, CH_3OH) *m/z* 479.8 $[M+H]^+$; anal. calcd for $C_{30}H_{36}N_6$, 5.5 HCl, 2.1 H_2O: C 50.1, H 6.36, N 11.69, found: C 50.1, H 6.38, N 11.36.

2,10-Di-[(4-(imidazol-4-yl)-ethyl)aminomethyl]dibenzo[*b,j*]-[*1,7*]phenanthroline 7 was obtained from dibenzo[*b,j*]-[*1,7*]phenanthroline-2,10-dicarboxaldehyde (100 mg, 0.297 mmol) and histamine (69.46 mg, 0.625 mmol) to yield 72.2 mg of a yellow powder (40%). ^{1}H NMR (200 MHz, D_2O/DCl): δ = 3.2 (m, 4H), 3.45 (m, 4H), 4.42 (s, 2H), 4.54 (s, 2H), 7.3 (s, 2H), 7.7 (d, J = 9.1 Hz, 1H), 7.83 (d, J = 9 Hz, 1H), 8.05 (s, 3H), 8.07 (t, J = 9 Hz, 2H), 8.4 (s, 1H), 8.05 (s, 2H), 8.7 (s, 1H), 10 ppm (s, 1H); MS (ESI, CH_3OH) *m/z* 527.4 $[M+H]^+$, 264.4 $[M+2H]^{2+}$.

2,10-Di-[(2-(piperidin-1-yl)ethyl)aminomethyl]dibenzo[*b,j*]-[*1,7*]phenanthroline 8 was obtained from dibenzo[*b,j*]-[*1,7*]phenanthroline-2,10-dicarboxaldehyde (150 mg, 0.446 mmol) and 1-(2-aminoethyl)piperidine (636 μL, 4.46 mmol) to yield 75 mg of a green powder (20%). Salt decomposition: 260 °C; ^{1}H NMR (200 MHz, D_2O/DCl): δ = 1.7–1.9 (m, 12H), 2.95–3.05 (m, 4H), 3.5–3.65 (m, 12H), 4.49 (s, 2H), 4.57 (s, 2H), 7.72 (d, J = 9 Hz, 1H), 7.83 (d, J = 9 Hz, 1H), 8.01 (s, 1H), 8.06 (s, 2H), 8.16 (d, J = 7.5 Hz, 1H), 8.23 (s, 1H), 8.4 (s, 1H), 8.63 (s, 1H), 10.01 ppm (s, 1H); MS (ESI, CH_3OH) *m/z* 561.5 $[M+H]^+$; anal. calcd for $C_{36}H_{44}N_6$, 5.5 HCl, 2.5 H_2O: C 53.61, H 6.76, N 10.42, found: C 53.84, H 6.77, N 10.04; UV/Vis (H_2O, pH ≈ 6.0): λ_{max} (ε [$M^{-1}cm^{-1}$]): 244 (53000), 313 (37000), 328 (45600), 350 nm (18000).

2,10-Di-[2-*N*-[di-(2-aminoethyl)]ethylaminomethyl]dibenzo[*b,j*]-[*1,7*]phenanthroline 9 was obtained from dibenzo[*b,j*]-[*1,7*]phenanthroline-2,10-dicarboxaldehyde (400 mg, 1.19 mmol) and 2-{bis-[2-(*tert*-butoxycarbonylamino)ethyl]}diaminoethane (1.03 g, 2.97 mmol). The crude product was first purified by flash chromatography on silica gel with $CH_2Cl_2/CH_3OH/NH_4OH$ 28% (85:10:5). The residue obtained was dissolved in chloroform (20 mL). The unreacted amines were treated with di-*tert*-butyl bicarbonate (1.18 mL, 5.13 mmol) added dropwise over 1 h in an ice bath. The solution was stirred for 2 h at room temperature, and the solvent was distilled off. The residue obtained was purified by flash chromatography on silica gel with CH_2Cl_2/CH_3OH (95:5). The chromatographic fractions were evaporated and dissolved in methanol (15 mL). Concentrated HCl (12 N, 10 mL) was added to deprotect the amine groups and give a chloride salt. Ether was added to precipitate the salt to yield 376 mg of a yellow powder (33%). ^{1}H NMR (200 MHz, D_2O/DCl): δ = 1.63 (t, J = 5.8 Hz, 8H), 1.84 (t, J = 7 Hz, 8H), 1.92 (s, 8H), 2.79 (s, 4H), 6.48–6.6 (m, 4H), 6.81 (s, 1H), 6.88–6.93 (m, 2H), 7.04 (d, J = 9 Hz, 1H), 8.06 (s, 1H), 9.46 ppm (s, 1H); MS (ESI, H_2O) *m/z* 597.5 $[M+H]^+$, 299.4 $[M+2H]^{2+}$; anal. calcd for $C_{34}H_{48}N_{10}$, 8.4 HCl, 3 H_2O: C 42.65, H 6.52, N 14.63, found: C 42.69, H 6.53, N 14.06.

2,10-Di-[(2-indoloethyl)aminomethyl]dibenzo[*b,j*]-[*1,7*]phenanthroline 10 was obtained from dibenzo[*b,j*]-[*1,7*]phenanthroline-2,10-dicarboxaldehyde (100 mg, 0.297 mmol)

and 2-aminoethylindole (104.9 mg, 0.624 mmol) to yield 33.4 mg of a yellow powder (14%). ^{1}H NMR (200 MHz, [D$_6$]DMSO): δ = 3.5–3.25 (m, 4H), 3.25–3.35 (m, 4H), 4.5 (s, 2H), 4.57 (s, 2H), 6.9–7.1 (m, 4H), 7.23 (s, 2H), 7.35 (d, J = 10.5 Hz, 2H), 7.57 (d, J = 10.5 Hz, 2H), 8.21 (d, J = 11 Hz, 2H), 8.4–8.5 (m, 4H), 8.67 (d, J = 9.5 Hz, 1H), 8.83 (s, 1H), 9.23 (s, 1H), 10.61 ppm (s, 1H); MS (ESI, CH_3OH) m/z 624.9 $[M+H]^+$; anal. calcd for $C_{42}H_{36}N_6$, 3.5 HCl, 2.5 H_2O: C 63.25, H 5.58, N 10.54, found: C 63.07, H 5.51, N 10.02.

2,10-Di-[(3-(imidazol-1-yl)propyl)aminomethyl]dibenzo[*b,j*]-[*1,7*]phenanthroline 12 was obtained from dibenzo[*b,j*]-[*1,7*]phenanthroline-2,10-dicarboxaldehyde (100 mg, 0.297 mmol) and 1-(3-aminopropyl)imidazole (74.58 μL, 0.625 mmol) to yield 75 mg of a yellow powder (32%). ^{1}H NMR (200 MHz, D_2O/DCl): δ = 2.3–2.5 (m, 4H), 3.2–3.3 (m, 4H), 4.34 (s, 6H), 4.47 (s, 2H), 7.38–7.51 (m, 5H), 7.67–7.97 (m, 6H), 8.07 (d, J = 9.1 Hz, 1H), 8.27 (s, 1H), 8.47 (s, 1H), 8.74 (s, 1H), 9.73 ppm (s, 1H); MS (ESI, CH_3OH) m/z 555.8 $[M+H]^+$; anal. calcd for $C_{34}H_{34}N_8$, 4.9 HCl, 3 H_2O: C 51.85, H 5.7, N 14.23, found: C 51.94, H 5.64, N 13.09.

2,10-Di-{[(3-*N*-(3-aminopropyl)-3′-*N*-methyl]propylaminomethyl}dibenzo[*b,j*][*1,7*]phenanthroline 13 was obtained from dibenzo[*b,j*][*1,7*]phenanthroline-2,10-dicarboxaldehyde (100 mg, 0.297 mmol) and 3-*N*-[3-(*tert*-butoxycarbonylamino)propyl]-3′-*N*-methyl-diaminopropane (315 mg, 1.285 mmol). The crude product was purified by flash chromatography on silica gel with CH_2Cl_2/CH_3OH/NH_4OH 28% (85:10:5) to yield 101.9 mg of a yellow powder (43%) corresponding to the bis-protected derivative of **13**. This powder (46.9 mg, 0.059 mmol) was dissolved in methanol (15 mL). HCl (1 N, 1 mL) was added, and the mixture was stirred overnight at room temperature. The solvent was evaporated, and the residue was dissolved in methanol. Ether and ethanol were added to precipitate **13** to yield 32.5 mg (57%) of a yellow powder. ^{1}H NMR (200 MHz, D_2O/DCl): δ = 2.02–2.15 (m, 8H), 2.8 (s, 3H), 2.81 (s, 3H), 2.96 (t, J = 7.5 Hz, 4H), 3.18–3.21 (m, 12H), 4.41 (s, 2H), 4.5 (s, 2H), 7.72 (d, J = 9 Hz, 1H), 7.82 (d, J = 8.88 Hz, 1H), 8.01 (s, 3H), 8.14 (d, J = 8.86 Hz, 1H), 8.23 (d, J = 9.52 Hz, 1H), 8.38 (s, 1H), 8.73 (s, 1H), 10.1 ppm (s, 1H); MS (ESI, H_2O) m/z 298.43 $[M+2H]^{2+}$; anal. calcd for $C_{36}H_{50}N_8$, 7.8 HCl, 4.1 H_2O: C 45.35, H 6.93, N 11.75, found: C 45.34, H 6.95, N 11.3; UV/Vis (H_2O, pH ≈ 6.0): λ_{max} (ε [M^{-1}cm^{-1}]): 243 (63400), 312 (60200), 327 (46900), 345 nm (24200).

2,10-Di-[(3-(morpholin-1-yl)propyl)aminomethyl]dibenzo[*b,j*]-[*1,7*]phenanthroline 14 was obtained from dibenzo[*b,j*]-[*1,7*]phenanthroline-2,10-dicarboxaldehyde (100 mg, 0.297 mmol) and 4-(3-aminopropyl)morpholine (91.32 μL, 0.625 mmol) to yield 112.4 mg of a yellow powder (44%). ^{1}H NMR (200 MHz, D_2O/DCl): δ = 2.2–2.3 (m, 4H), 3.25–3.29 (m, 12H), 3.45–3.55 (m, 4H), 3.7–3.8 (m, 4H), 3.95–4.05 (m, 4H), 4.37 (s, 2H), 4.49 (s, 2H), 7.35 (d, J = 9.14 Hz, 1H), 7.68–7.94 (m, 6H), 8.22 (s, 1H), 8.35 (s, 1H), 9.53 ppm (s, 1H); MS (ESI, CH_3OH) m/z 593.5 $[M+H]^+$, 297.25 $[M+2H]^{2+}$; anal. calcd for $C_{36}H_{44}N_6O_2$, 5 HCl, 4.6 H_2O: C 50.39, H 6.78, N 9.79, O 12.31, found: C 50.51, H 6.45, N 9.37, O 12.64.

2,10-Di-[(4-aminobutyl)aminomethyl]dibenzo[*b,j*]-[*1,7*]phenanthroline 15 was obtained from dibenzo[*b,j*]-[*1,7*]phenanthroline-2,10-dicarboxaldehyde (150 mg, 0.446 mmol) and 4-(*tert*-butoxycarbonylamino)butylamine (209.8 mg, 1.115 mmol) to yield 100.9 mg of a yellow powder (30%). ^{1}H NMR (200 MHz, D_2O/DCl): δ = 1.67–1.69 (m, 8H), 2.92 (t, J = 6 Hz, 4H), 3.09 (q, J = 7.3 Hz, 4H), 4.35 (s, 2H), 4.42 (s, 2H), 7.67 (d, J = 9.2 Hz, 1H), 7.77 (d, J = 9.12 Hz, 1H), 7.89 (d, J = 9 Hz, 1H), 7.97 (s, 2H), 8.11 (t, J = 7.6 Hz, 2H), 8.26 (s, 1H), 8.67 (s, 1H), 9.88 ppm (s, 1H); MS (ESI, H_2O) m/z 481.26 $[M+H]^+$, 241.34 $[M+2H]^{2+}$; anal. calcd for $C_{30}H_{36}N_6$, 6 HCl, 2 H_2O: C 48.98, H 6.25, N 11.42, found: C 48.98, H 6.45, N 10.82.

7-[*n*-propylaminomethyl]dibenzo[*b,j*][*1,7*]phenanthroline 16 was obtained from dibenzo[*b,j*][*1,7*]phenanthroline-7-carboxaldehyde **24** (15 mg, 0.048 mmol) and *n*-propylamine (1 mL, 12.17 mmol). After $NaBH_4$ treatment, the crude product was purified by flash chromatography on silica gel with CH_2Cl_2/CH_3OH (90:10) to yield 18 mg of a green powder (80%). ^{1}H NMR (300 MHz, [D$_4$]MeOD/CD_2Cl_2 1:1): δ = 1.13 (t, J = 7.3 Hz, 3H), 1.95 (s, J = 8.4 Hz, 2H), 3.39 (t, J = 7.9 Hz, 4H), 5.05 (s, 2H), 7.83 (t, J = 7.2 Hz, 1H), 7.95 (t, J = 7.5 Hz, 1H), 8.05 (t, J = 7.2 Hz, 1H), 8.2 (t, J = 8.1 Hz, 1H), 8.25 (s, 1H), 8.33 (d, J = 7.8 Hz, 1H), 8.38 (d, J = 8.4 Hz, 1H), 8.44 (d, J = 8.7 Hz, 1H), 8.55 (d, J = 8.1 Hz, 1H), 9.37 (s, 1H), 10.68 ppm (s, 1H); MS (ESI, CH_3OH) m/z 352 $[M+H]^+$; anal. calcd for $C_{24}H_{21}N_3$, 3 HCl, 0.1 H_2O: C 62.29, H 5.23, N 9.08, found: C 62.25, H 5.57, N 8.83.

2,7,10-Tri-[*n*-propylaminomethyl]dibenzo[*b,j*][*1,7*]phenanthroline 17: SeO_2 (340 mg, 3.07 mmol) was added to a mixture of trimethylquinacridine **25** (85 mg, 0.26 mmol) and naphthalene (1 g). After heating at reflux for 2.5 h, the mixture was cooled to 70 °C and filtered. The solid collected was thoroughly washed with a mixture of CH_3OH/CH_2Cl_2 (1:4); solvents were mixed together and removed under reduced pressure. The solid was washed with pentane (3 times); after the solvent was removed, it was dried under reduced pressure. Tris-carboxaldehyde derivatives were obtained as a brown powder (93 mg, 96% chemical yield). The amine (40 equiv) to be introduced as side chain was added to a solution of the previously prepared tris-carboxaldehyde derivatives (50 mg, 0.13 mmol) in CH_3OH/CH_2Cl_2 (1:4). The mixture was stirred at room temperature until the complete disappearance of the aldehyde signals, as monitored by ^{1}H NMR. The solvents were distilled off, and the crude tris-imine was dissolved in methanol, then cooled to 0 °C. $NaBH_4$ (4 equiv) was added, and the solution was stirred at 0 °C for 2 h and at room temperature for 30 min. The solvent was distilled off and water (2 mL) was added. The product was then extracted with CH_2Cl_2. The organic layer was dried over $MgSO_4$, filtered, and evaporated. The residue obtained was dissolved in CH_3OH, and HCl (1 N) was added to give a chloride salt, which was precipitated by the addition of THF. The salt was finally crystallized from EtOH/HCl (1 N) to yield to the desired product under pure form as an orange powder (9.8 mg, 14% chemical yield over two steps). ^{1}H NMR (300 MHz, D_2O): δ = 0.59–0.74 (m, 9H), 1.33–1.63 (m, 6H), 2.77 (d, J = 7.8 Hz, 2H), 2.88 (d, J = 8.1 Hz, 2H), 3.08 (t, J = 8.1 Hz, 2H), 4.09 (s, 2H), 4.31 (s, 2H), 4.73 (s, 2H), 7.30 (d, J = 2.1 Hz, 1H), 7.81–7.88 (m, 3H), 7.96 (dd, J = 9.0, 1.8 Hz, 1H), 8.31 (s, 1H), 8.91 (s, 1H), 9.97 ppm (s, 1H); MS (ESI, CH_3OH/DMSO) m/z 494 $[N+H]^+$; HRMS (ESI, CH_3OH/DMSO): 494.3328 ($C_{32}H_{40}N_5$, calcd: 494.3284).

2,10-Di-[(*n*-propylaminoethyl)aminomethyl]-5-*N*-methyldibenzo-[*b,j*][*1,7*]phenanthroline 18 was obtained from dibenzo[*b,j*]-[*1,7*]phenanthroline-2,10-dicarboxaldehyde **22** (300 mg, 0.892 mmol) and *n*-propylamine (20 mL). The solid obtained was suspended in CH_2Cl_2 (100 mL). A solution of di-*tert*-butyl carbonate anhydride (2 mL, 8.92 mmol) in dry CH_2Cl_2 (100 mL) was added dropwise over 1 h. The solution was after stirred for 1 h. The organic layer was extracted with water, dried over $MgSO_4$, and evaporated. The crude product was purified by flash chromatography on silica gel with CH_2Cl_2/CH_3OH (98:2). The chromatographic fractions were evaporated and dissolved in CH_2Cl_2. Pentane was added to precipitate a first intermediate to yield 386 mg of a yellow powder (69.5%). ^{1}H NMR (300 MHz, $CDCl_3$): δ = 0.87 (br s, 6H), 1.52 (br s, 22H), 3.19 (br s, 2H), 3.29 (br s, 2H), 4.67 (s, 4H), 7.75 (br s, 2H), 7.79 (s, 1H), 7.92 (s, 2H), 7.98 (s, 1H), 8.24 (d, J =

8.7 Hz, 1H), 8.31 (d, $J=8.7$ Hz, 1H), 8.53 (s, 1H), 10.1 ppm (s, 1H); MS (ESI+, CH_3OH) m/z 623 $[M+H]^+$. This intermediate (386 mg, 0.62 mmol) in 1,2-dichloroethane (20 mL) was held at reflux under nitrogen. Methyl triflate (140 μL, 1.24 mmol) was added dropwise over 15 min, and the solution was stirred for 1 h. After cooling to room temperature, the solvent was removed under vacuum, and the yellow solids were suspended in CH_2Cl_2. The crude product was purified by flash chromatography on silica gel with CH_2Cl_2/CH_3OH (95:5). The chromatographic fractions were evaporated and dissolved in CH_2Cl_2. Pentane was added to precipitate a second intermediate to yield 231 mg of a yellow powder (47%). ^{1}H NMR (300 MHz, $CDCl_3$): $\delta=0.91$ (q, $J=7.2$ Hz, 6H), 1.45 (br s, 4H), 1.57 (br s, 18H), 3.29 (br s, 4H), 4.73 (s, 2H), 4.79 (s, 2H), 5.05 (s, 3H), 7.92 (d, $J=9.9$ Hz, 1H), 7.96 (s, 1H), 8.3 (d, $J=9$ Hz, 1H), 8.4 (s, 2H), 8.45 (d, $J=8.9$ Hz, 1H), 8.74 (d, $J=10.2$ Hz, 1H), 8.91 (s, 1H), 10.92 ppm (s, 1H); MS (ESI+, CH_3OH) m/z 637 $[M+H]^+$. HCl (12 N, 5 mL) was added to a solution of this second intermediate (100 mg, 0.127 mmol) in CH_3OH (20 mL), and the mixture was stirred for 20 min at room temperature. The solution was concentrated, and ether was added to obtain **18** (70 mg) as an orange powder (100%). ^{1}H NMR (300 MHz, D_2O/DCl): $\delta=0.07$–013 (m, 6H), 0.87–0.96 (m, 4H), 2.33 (q, $J=7.8$ Hz, 4H), 3.79 (s, 2H), 3.84 (s, 2H), 4.13 (s, 3H), 7.65 (dd, $J=11.1$, 1.8 Hz, 1H), 7.78 (dd, $J=11.4$, 2.4 Hz, 1H), 7.91 (d, $J=9.6$ Hz, 1H), 7.93 (s, 1H), 7.97 (d, $J=9.3$ Hz, 1H), 8.08 (s, 1H), 8.1 (d, $J=9.9$ Hz, 1H), 9.23 (s, 1H), 10.51 ppm (s, 1H); MS (ESI+, CH_3OH) m/z 219 $[M+H]^+$; anal. calcd for $C_{29}H_{33}N_4$, 3.5 HCl, 1 H_2O: C 59.65, H 6.59, N 9.59, found: C 59.46, H 6.54, N 9.32.

5-*N*-Methyl-2,10-dimethyldibenzo[*b,j*][*1,7*]phenanthroline 19 was obtained from 2,10-dimethyldibenzo[*b,j*][*1,7*]phenanthroline **22** (50 mg, 0.162 mmol); a solution of **22** in CH_2Cl_2 (10 mL) was heated at reflux under nitrogen. Methyl triflate (73.5 μL, 0.65 mmol) was added dropwise over 15 min, and the solution was stirred for 1 h. After cooling to room temperature, the solvent was removed under vacuum, and the crude product was purified by flash chromatography on silica gel with CH_2Cl_2/CH_3OH (90:10). The chromatographic fractions were evaporated and dissolved in CH_2Cl_2 (5 mL). Pentane was added to precipitate the desired product to yield 27.1 mg of a yellow powder (34%). ^{1}H NMR (300 MHz, [D_6]DMSO): $\delta=2.64$ (s, 3H), 2.71 (s, 3H), 4.88 (s, 3H), 7.96 (d, $J=$ 8.85 Hz, 1H), 8.12 (s, 1H), 8.33 (t, $J=9.9$ Hz), 8.61 (d, $J=10.2$ Hz, 1H), 8.69 (s, 1H), 8.75 (d, $J=9.3$ Hz, 1H), 8.85 (d, $J=9.9$ Hz, 1H), 9.24 (s, 1H), 10.86 ppm (s, 1H); MS (CI+, CH_3OH/$CHCl_3$ 1:1) m/z 323 $[M]^+$; anal. calcd for $C_{24}H_{19}F_3N_2O_3S$, 0.1 CH_2Cl_2: C 60.43, H 3.99, N 5.82, found: C 60.2, H 4.06, N 5.69.

8-Chloro-5-*N*-methyl-2,10-dimethyldibenzo[*b,j*]-[*1,7*]phenanthroline 20 was obtained from dichloro-2,10-dimethyldibenzo[*b,j*][*1,7*]phenanthroline **23** (5.66 g, 15 mmol); a solution of **23** in dry THF (173 mL) was added under nitrogen to a solution of $LiAlH_4$ (1.14 g, 30 mmol) in dry THF (173 mL). The mixture was held at reflux overnight, and the blue solution was cooled to room temperature. After cooling to 4 °C, water (1 mL), NaOH (1 mL, 15%) and water (3 mL) were added sequentially. The mixture was vigorously stirred for 20 min and filtered. The precipitate was washed with CH_2Cl_2, and the filtrate was then dried under $MgSO_4$ and concentrated. This mixture was held at reflux overnight in ethanol (157 mL) with $FeCl_3{\cdot}6H_2O$ (19.67 g, 72.77 mmol) first dissolved in water (135 mL). NH_4OH (50 mL, 15%) was added to the dark solution, and the black precipitate was filtered and washed with methanol. The alcoholic solvents were removed under vacuum, and the remaining water was extracted with CH_2Cl_2. The organic layer was dried over $MgSO_4$ and evaporated. The brown residues were purified by flash chromatography on silica gel with CH_2Cl_2/CH_3OH (99:1). The chromatographic fractions were mixed and evaporated, and pentane was added to precipitate the product to yield 2.95 g of a yellow powder (57%). ^{1}H NMR (200 MHz, $CDCl_3$): $\delta=2.64$ (s, 6H), 7.68 (t, $J=7.2$ Hz, 2H), 7.89 (s, 1H), 7.98 (d, $J=$ 9.9 Hz, 1H), 8.11 (s, 1H), 8.18 (d, $J=8.74$ Hz, 2H), 8.32 (d, $J=9.6$ Hz, 1H), 9.9 ppm (s, 1H); MS (CI+, CH2L2) m/z 343 $[M+H]^+$; anal. calcd for $C_{22}H_{15}N_2Cl$, 0.14 CH_2Cl_2: C 74.96, H 4.31, N 7.9, found: C 74.73, H 4.54, N 8.27. This product (35.2 mg, 0.102 mmol) in CH_2Cl_2 (10 mL) was held at reflux under nitrogen. Methyl triflate (51.7 μL, 0.308 mmol) was added dropwise over 15 min, and the solution was stirred for 1 h. After cooling to room temperature, the solvent was removed under vacuum, and the yellow solids were suspended in CH_2Cl_2 (5 mL). Pentane was added to precipitate **20** to yield 38.5 mg of a yellow powder (74%). ^{1}H NMR (300 MHz, [D_6]DMSO): $\delta=2.69$ (s, 3H), 2.71 (s, 3H), 4.89 (s, 3H), 8.01 (dd, $J=9$, 1.8 Hz, 1H), 8.27 (s, 1H), 8.34 (dd, $J=9$, 3.3 Hz, 2H), 8.66 (s, 1H), 8.72 (t, $J=10.5$ Hz, 2H), 8.92 (d, $J=10.2$ Hz, 1H), 10.79 ppm (s, 1H); MS (CI^+, CH_3OH/$CHCl_3$ 1:1 *v/v*) m/z 356.9 $[M]^+$; anal. calcd for $C_{24}H_{18}N_2F_3SO_3Cl$: C 56.86, H 3.55, N 5.52, found: C 56.75, H 3.61, N 5.37.

Assay for short-term inhibition of tumor cell growth: Cells were plated in 96-well plates and treated with various concentrations of compound (0.03, 0.1, 0.3, 1, 3, and 10 μM). The MTT assay was used to determine drug-mediated cytotoxicity after four days of treatment. The number of surviving cells is directly proportional to the level of the formazan product created. The color can then be quantified using a simple colorimetric assay. The MTT [3-(4,5-dimethylthiazol-2-yl)-2,5-diphenyltetrazolium bromide] assay, first described by Mosmann in 1983,[24] is based on the ability of a mitochondrial dehydrogenase enzyme from viable cells to cleave the tetrazolium rings of the pale-yellow MTT to form dark-blue formazan crystals, which are largely impermeable to cell membranes, thus resulting in its accumulation within healthy cells. Lysis of the cells by addition of a detergent results in the liberation of the crystals which are solubilized. The number of surviving cells is directly proportional to the level of the formazan product created. The color can then be quantified with a simple colorimetric assay. The results can be read on a multi-well scanning spectrophotometer (ELISA reader).

NMR spectroscopy and modeling studies: The heptamer d-(TTAGGGT) was purchased purified from Eurogentec. The d-[(TTAGGGT)]$_4$ NMR sample, in 100 mM KCl and 10 mM K_2HPO_4, was heated at 80 °C for 5 min, and then gradually cooled to room temperature. The sample was checked by circular dichroism, and the concentration was measured by UV/Vis at $\lambda=260$ nm. The final concentration of the NMR sample was 1.3 mM. Known amounts of **1** were then added to the NMR tube until a 2:1 stoichiometry was reached.

NMR spectroscopy: NMR experiments were carried out using a Varian Unity+ 500 MHz spectrometer. Proton sequential assignments were achieved by analysis of *z*-filtered TOCSY and NOESY experiments registered at 318 K. The TOCSY spectra were recorded with a spin-lock time of 80 ms, and NOESY spectra were recorded with various mixing times (400, 250, and 110 ms). All 2D NMR experiments were recorded with 512 ($t1$)×2048 ($t2$) complex data points. 128 scans were acquired over a spectra width of 5000 Hz in both dimensions for samples in D_2O and 8000 Hz for H_2O/D_2O (90:10) samples. Water resonance was suppressed either by standard presaturation or by the sculpting gradients scheme using selective pulses of 3–4 ms. Data processing and analysis were performed using the VNMR program (Varian) on a Sunray workstation.

Molecular modeling: Calculations were performed on a workstation using InsightII 2005 and Discover 2004.1 (Biosym/Molecular Simulation). The energy of the system was calculated with the amber force field.[26] A distance-dependent dielectric constant $\varepsilon = 4r$ was used to account for solvent effect. A starting structure of the intermolecular parallel quadruplex was constructed using the Biopolymer module of InsightII. The two intercalation sites between A_3 and G_4 quartets and between the G_6–T_7 steps were created using an axial rise of 6.5 Å and a twist angle of 36°. Potassium ions were added all along the phosphate backbone using the "counterion" program of Insight and two others were manually placed equidistantly from the G_4 and G_5 quartets and the G_5 and G_6 quartets in the central cavity of the quadruplex. Compound **1** was then manually docked into the pre-existing intercalation sites, and four different starting structures were generated using the AFFINITY docking program of InsightII. These structures served as starting structures for the following restrained molecular dynamics protocol.

Intermolecular NOE were classified semi-quantitatively into three categories: strong (1.8–3.0 Å), medium (2.5–4.0 Å) and weak (3.5–5.0 Å), and then introduced as restraints for the calculations. However, due to the paucity of NOE restraints, the 5′ part of the duplex T_1T_2 and the G_5 quartet were fixed, limiting the dynamics calculation to the two binding sites only. The complex was then initially minimized using 100 and 2000 cycles of steepest descent and conjugate gradients, respectively. Then a 100-ps simulated annealing dynamics under restrained conditions was performed: the system was first heated to 400 K for 10 ps, then cooled to 250 K in 50-K steps. During cooling, 10-ps dynamics was done at each step. At 250 K, a final dynamics was run for 80 ps. Six structures were randomly chosen over the last 20 ps, averaged, and then energy-minimized. The four generated structures were averaged and energy-minimized to generate the final complex structure. No violations greater than 0.1 Å were detected.

Acknowledgements

This work was supported by grants from ARC (#3365), E.U. FP6 "MolCancerMed" (LSHC-CT-2004-502943 to J.L.M.) and Ligue Nationale Contre le Cancer (to C.H.). The authors gratefully acknowledge Anne De Cian, Laurent Lacroix, Jean-Francois Riou, and Patrick Mailliet for helpful discussions, Jérôme Bernardi for his participation at the early stage of the NMR study, and Ermira Pazzoli for reading the manuscript.

Keywords: DNA structures · electrostatic interactions · NMR spectroscopy · quinacridines · stacking interactions

[1] a) E. H. Blackburn, *Nature* **2000**, *408*, 53; b) D. Liu, M. S. O'Connor, J. Qin, Z. Songyang, *J. Biol. Chem.* **2004**, *279*, 51338; c) A. Smogorzewska, T. de Lange, *Annu. Rev. Biochem.* **2004**, *73*, 177.

[2] S. Neidle, G. N. Parkinson, *Curr. Opin. Struct. Biol.* **2003**, *13*, 275.

[3] a) S. Burge, G. N. Parkinson, P. Hazel, A. K. Todd, S. Neidle, *Nucleic Acids Res.* **2006**, *34*, 5402; b) A. T. Phan, V. Kuryavyi, D. J. Patel, *Curr. Opin. Struct. Biol.* **2006**, *16*, 288; c) J. T. Davis, *Angew. Chem.* **2004**, *116*, 684; *Angew. Chem. Int. Ed.* **2004**, *43*, 668.

[4] a) D. Gomez, N. Aouali, A. Londono-Vallejo, L. Lacroix, F. Mégnin-Chanet, T. Lemarteleur, C. Douarre, K. Shin-ya, P. Mailliet, C. Trentesaux, H. Morjani, J.-L. Mergny, J.-F. Riou, *J. Biol. Chem.* **2003**, *278*, 50554; b) A. M. Burger, F. Dai, C. M. Schultes, A. P. Reszka, M. J. B. Moore, J. A. Double, S. Neidle, *Cancer Res.* **2005**, *65*, 1489; c) G. Pennarun, C. Granotier, L. R. Gauthier, D. Gomez, F. Hoffschir, E. Mandine, J.-F. Riou, J.-L. Mergny, P. Mailliet, F. Boussin, *Oncogene* **2005**, *24*, 2917; d) C. Douarre, D. Gomez, H. Morjani, J.-M. Zahm, M.-F. O'Donohue, L. Eddabra, P. Mailliet, J.-F. Riou, C. Trentesaux, *Nucleic Acids Res.* **2005**, *33*, 2192; e) D. Gomez, M.-F. O'Donohue, T. Wenner, C. Douarre, J. Macadre, P. Koebel, M. J. Giraud-Panis, H. Kaplan, A. Kolkes, K. Shin-ya, J.-F. Riou, *Cancer Res.* **2006**, *66*, 6908; f) D. Gomez, T. Wenner, B. Brassart, C. Douarre, M.-F. O'Donohue, V. El Khoury, K. Shin-ya, H. Morjani, C. Trentesaux, J.-F. Riou, *J. Biol. Chem.* **2006**, *281*, 38721.

[5] a) N. W. Kim, M. A. Piatyszek, K. R. Prowse, C. B. Harley, M. D. West, P. L. Ho, G. M. Corviello, W. E. Wright, S. L. Weinrich, J. W. Shay, *Science* **1994**, *266*, 2011; b) J. W. Shay, S. Bachetti, *Eur. J. Cancer* **1997**, *33*, 787.

[6] a) L. H. Hurley, *Nat. Rev. Cancer* **2002**, *2*, 188; b) S. Neidle, G. Parkinson, *Nat. Rev. Drug Discovery* **2002**, *1*, 383; c) E. M. Rezler, D. J. Bearss, L. H. Hurley, *Annu. Rev. Pharmacol. Toxicol.* **2003**, *43*, 359; d) S. Neidle, D. E. Thurston, *Nat. Rev. Cancer* **2005**, *5*, 285.

[7] E. W. White, F. Tanious, M. A. Ismail, A. P. Reszka, S. Neidle, D. W. Boykin, W. D. Wilson, *Biophys. Chem.* **2007**, *126*, 140.

[8] a) O. Baudoin, M.-P. Teulade-Fichou, J.-P. Vigneron, J.-M. Lehn, *J. Org. Chem.* **1997**, *62*, 5458; b) J.-L. Mergny, L. Lacroix, M.-P. Teulade-Fichou, C. Hounsou, L. Guittat, M. Hoarau, P. B. Arimondo, J.-P. Vigneron, J.-M. Lehn, J.-F. Riou, T. Garestier, C. Hélène, *Proc. Natl. Acad. Sci. USA* **2001**, *98*, 3062; c) M.-P. Teulade-Fichou, C. Carrasco, L. Guittat, C. Bailly, P. Alberti, J.-L. Mergny, A. David, J.-M. Lehn, W. D. Wilson, *J. Am. Chem. Soc.* **2003**, *125*, 4732; d) C. Allain, D. Monchaud, M.-P. Teulade-Fichou, *J. Am. Chem. Soc.* **2006**, *128*, 11890.

[9] S. M. Haider, G. N. Parkinson, S. Neidle, *J. Mol. Biol.* **2003**, *326*, 117.

[10] M. Kaiser, A. De Cian, M. Sainlos, C. Renner, J.-L. Mergny, M.-P. Teulade-Fichou, *Org. Biomol. Chem.* **2006**, *4*, 1049.

[11] A. Slama-Schwok, J. Jazwinski, A. Béré, T. Montenay-Garestier, M. Rougée, C. Hélène, J.-M. Lehn, *Biochemistry* **1989**, *28*, 3227.

[12] a) R. Lartia, H. Bertrand, M.-P. Teulade-Fichou, *Synlett* **2006**, 610; b) C. Jacquelin, N. Saettel, C. Hounsou, M.-P. Teulade-Fichou, *Tetrahedron Lett.* **2005**, *46*, 2589.

[13] a) J.-L. Mergny, J.-C. Maurizot, *ChemBioChem* **2001**, *2*, 124; b) A. De Cian, L. Guittat, M. Kaiser, B. Saccà, S. Amrane, A. Bourdoncle, P. Alberti, M.-P. Teulade-Fichou, L. Lacroix, J.-L. Mergny, *Methods* **2007**, in press, DOI: 10.1016/j.ymeth.2006.10.0004.

[14] The protonation of cyclic nitrogen atoms of *meta*-quinacridine has been shown not to occur at physiological pH (pK_a values of cyclic nitrogens of compound **1** have been determined: the first one has a pK_a value below 1 and the second one, a pKa value of 3.3, see reference [8a]). Thus, the indicated in situ charges correspond to the estimate of the global charges only held by the side chains (both proximal and distal amine groups). The pKa value of the benzylic nitrogen atoms (proximal amine groups) can be estimated by fluorimetric titration owing to a photoinduced electron-transfer effect from the lone pair of the benzylic nitrogen atom that quenches the fluorescence.[8a] Thus, for each compound, proximal amine charges were estimated on the basis of the pKa values collected with compounds **1**, **6**, **7**, **10**, and **11** by fluorescence. For the distal amine groups, the pKa data reported in the literature have been further taken into account to estimate the global in situ charges; see: a) J. Hine, F. Via, J. H. Hensen, *J. Org. Chem.* **1971**, *36*, 2926; b) M. Ciampolini, P. Paoletti, *J. Phys. Chem.* **1961**, *65*, 1224; c) F. Onasch, D. Aikens, S. Bunce, H. Schwartz, D. Nairn, C. Hurwitz, *Biophys. Chem.* **1984**, *19*, 245; d) A. Vacca, D. Arenare, P. Paoletti, *Inorg. Chem.* **1966**, *5*, 1384; e) M. I. Page, W. P. Jencks, *J. Am. Chem. Soc.* **1972**, *94*, 8818.

[15] a) R. J. Harrison, J. Cuesta, G. Chessari, M. Read, S. K. Basra, A. P. Reszka, J. Morrell, S. M. Gowan, C. M. Incles, F. A. Tanious, W. D. Wilson, L. R. Kelland, S. Neidle, *J. Med. Chem.* **2003**, *46*, 4463; b) C. M. Schultes, B. Guyen, J. Cuesta, S. Neidle, *Bioorg. Med. Chem. Lett.* **2004**, *14*, 4347; c) M. J. B. Moore, C. M. Schultes, J. Cuesta, F. Cuenca, M. Gunaratnam, F. A. Tanious, W. D. Wilson, S. Neidle, *J. Med. Chem.* **2006**, *49*, 581.

[16] a) O. Y. Fedoroff, M. Salazar, H. Han, V. V. Chemeris, S. M. Kerwin, L. H. Hurley, *Biochemistry* **1998**, *37*, 12367; b) J. T. Kern, P. W. Thomas, S. M. Kerwin, *Biochemistry* **2002**, *41*, 11379; c) E. Gavathiotis, R. A. Heald, M. F. G. Stevens, M. S. Searle, *Angew. Chem.* **2001**, *113*, 4885; *Angew. Chem. Int. Ed.* **2001**, *40*, 4749; d) E. Gavathiotis, R. A. Heald, M. F. G. Stevens, M. S. Searle, *J. Mol. Biol.* **2003**, *334*, 25; e) M. J. Cocco, L. A. Hanakahi, M. D. Huber, N. Maizels, *Nucleic Acids Res.* **2003**, *31*, 2944.

[17] A. T. Phan, V. Kuryavyi, H. Y. Gaw, D. Patel, *Nat. Chem. Biol.* **2005**, *1*, 167.

[18] a) W. Duan, A. Rangan, H. Vankayalapati, M.-Y. Kim, Q. Zeng, D. Sun, H. Han, O. Y. Fedoroff, D. Nishioka, S. Y. Rha, E. Izbicka, D. D. Von Hoff, L. H. Hurley, *Mol. Cancer Ther.* **2001**, *1*, 103; b) A. K. Mehta, Y. Shayo, H. Vankayalapati, L. H. Hurley, J. Schaefer, *Biochemistry* **2004**, *43*, 11953.
[19] A. Nicholls, K. A. Sharp, B. Honig, *Proteins Struct. Funct. Genet.* **1991**, *11*, 281.
[20] G. R. Clark, P. D. Pytel, C. J. Squire, S. Neidle, *J. Am. Chem. Soc.* **2003**, *125*, 4066.
[21] a) J. Ren, J. B. Chaires, *Biochemistry* **1999**, *38*, 16067; b) F. Rosu, E. De Pauw, L. Guittat, P. Alberti, L. Lacroix, P. Mailliet, J.-F. Riou, J.-L. Mergny, *Biochemistry* **2003**, *42*, 10361.
[22] D. Monchaud, C. Allain, M.-P. Teulade-Fichou, *Bioorg. Med. Chem. Lett.* **2006**, *16*, 4842.
[23] A. De Cian, L. Guittat, K. Shin-ya, J.-F. Riou, J.-L. Mergny, *Nucleic Acids Symp. Ser.* **2005**, *49*, 235.
[24] T. Mosmann, *J. Immunol. Methods* **1983**, *65*, 55.
[25] a) C. Schaffitzel, I. Berger, J. Postberg, J. Hanes, H. J. Lipps, A. Pluckthun, *Proc. Natl. Acad. Sci. USA* **2001**, *98*, 8572; b) J. C. Darnell, K. B. Jensen, P. Jin, V. Brown, S. T. Warren, R. B. Darnell, *Cell* **2001**, *107*, 489; c) M. L. Duquette, P. Handa, J. A. Vincent, A. F. Taylor, N. Maizels, *Gen. Dev.* **2004**, *18*, 1618; d) K. Paeschke, T. Simonsson, J. Postberg, D. Rhodes, H. J. Lipps, *Nat. Struct. Mol. Biol.* **2005**, *12*, 847; e) C. Granotier, G. Pennarun, L. Riou, F. Hoffschir, L. R. Gauthier, A. De Cian, D. Gomez, E. Mandine, J.-F. Riou, J.-L. Mergny, P. Mailliet, B. Dutrillaux, F. D. Boussin, *Nucleic Acids Res.* **2005**, *33*, 4182; f) J. Eddy, N. Maizels, *Nucleic Acids Res.* **2006**, *34*, 3887.
[26] S. J. Weiner, P. A. Kollman, D. T. Nguyen, D. A. Case, *J. Comput. Chem.* **1986**, *7*, 230.

Received: December 8, 2006
Revised: February 16, 2007
Published online on March 27, 2007

